JOC The Journal of Organic Chemistry

pubs.acs.org/joc Article

Solid-Phase Synthesis of Sequence-Defined Informational Oligomers

Kyle R. Strom and Jack W. Szostak*

Cite This: J. Org. Chem. 2020, 85, 13929−13938

Read Online

ACCESS | Metrics & More | Article Recommendations | Supporting Information

ABSTRACT: Genetic biopolymers utilize defined sequences and monomer-specific molecular recognition to store and transfer information. Synthetic polymers that mimic these attributes using reversible covalent chemistry for base-pairing pose unique synthetic challenges. Here, we describe a solid-phase synthesis methodology for the efficient construction of ethynyl benzene oligomers with specific sequences of aniline and benzaldehyde subunits. Handling these oligomers is complicated by the fact that they often exhibit multiple conformations because of intra- or intermolecular pairing. We describe conditions that allow the dynamic behavior of these oligomers to be controlled so that they may be manipulated and characterized without needing to mask the recognition units with protecting groups.

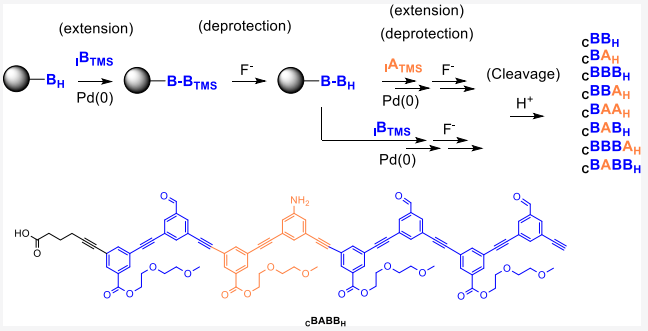

INTRODUCTION

In genetic polymers, molecular recognition between complementary nucleotides is the chemical basis for self-replication and self-assembly. In all known living things, purine and pyrimidine nucleobases function as the recognition units in base-pairing interactions and allow parent polymers to transfer information to their daughter polymers.[1] The canonical nucleobases of DNA and RNA (A, G, C, T, and U), and nearly all synthetic XNAs,[2] utilize patterns of hydrogen-bond donors and acceptors to give specificity to their base-pairing interactions. Although inefficient, the demonstrated enzyme-free copying of these biopolymers suggests that the information transfer function is intrinsic to the polymer structure and is not entirely dependent on the complex biomachinery of living systems.[3−6] Alternative synthetic systems that use reversible covalent chemistry to form base pairs could conceivably share the ability of biological genetic polymers to store and propagate information and to self-assemble into higher-order functional structures. Ultimately, it may be possible to develop such synthetic polymers into systems that can mimic the greatest aspect of natural biopolymers, namely, the spontaneous development and refinement of function through genetic evolution.[7]

Recently, we described a synthetic system capable of information storage and self-replication; two dimers with sequence-defined aniline (A) and benzaldehyde (B) subunits capable of templating the synthesis of their sequence-complementary daughters through reversible covalent imine bonds (Figure 1a).[8] Concurrent with our work, Hunter and co-workers reported a trimer with sequence-defined phenol (P) and benzoic acid (N) subunits capable of templating the synthesis of its complementary trimer through reversible covalent ester linkages (Figure 1b).[9] These demonstrations build on several examples of templated polymerization in which the length and structure of the daughter polymers are controlled by the length of a parent template.[10,11] A particularly notable example is the templated ring-opening metathesis polymerization of ester-linked cyclic olefins recently reported by Zhou and Palermo.[12] Although this work demonstrates the exceptional control of polymerization products that can be achieved using templates, sequence information is not transferred in this system as the parent oligomers are oligothiophene homopolymers and do not encode sequence information.

To our knowledge, the examples reported by us and by Hunter *et al.* are the first examples to demonstrate the transfer of sequence information through reversible covalent chemistry. These two systems are markedly distinct in their molecular structures and in the chemistries they employ: for backbone synthesis, Sonogashira coupling *versus* azide−alkyne cycloaddition, and for base pair formation, imine bonds *versus* ester bonds. These differences may indicate the existence of an expansive chemical space of genetic polymers that is distant from the nucleotides of biology and that is nearly unexplored.

The study of sequence-defined polymers functionalized with subunits amenable to reversible covalent interactions has been limited by the lack of synthetic methods for their construction

Received: August 16, 2020
Published: October 16, 2020

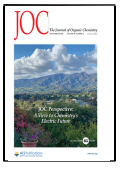

https://dx.doi.org/10.1021/acs.joc.0c01977
J. Org. Chem. 2020, 85, 13929−13938

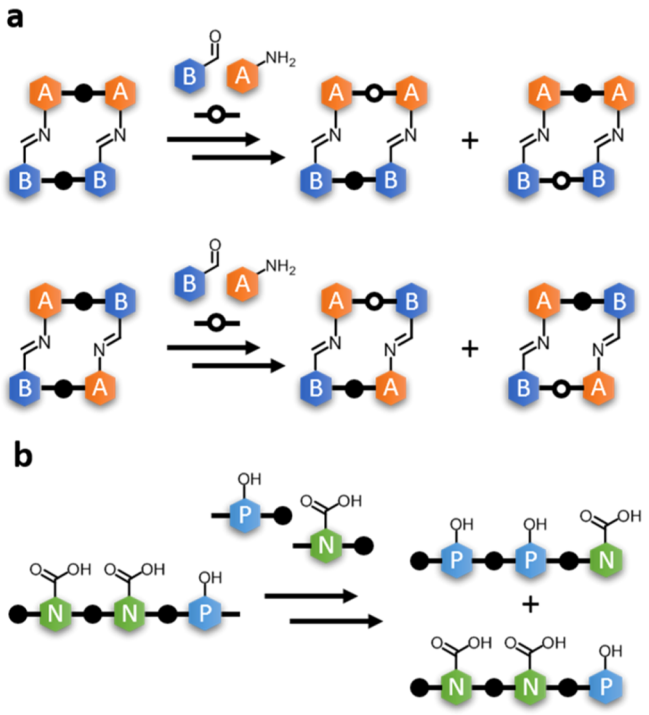

Figure 1. Sequence information transfer using reversible covalent chemistry. (a) Template copying of sequence-defined macrocycles through transimination and linking of monomers. (b) Template copying of a sequence-defined trimer through ester bond formation, polymerization, and hydrolysis.

and a poor understanding of how to control their dynamic behavior so that they may be easily manipulated once in hand. Although great strides have been made in developing methods to build long sequence-defined informational polymers,[13,14] the complexity resulting from the presence of the coreactive functional groups necessary for sequence recognition has limited the synthetic accessibility of such oligomers. The synthesis of sequence-defined oligoarylacetylenes with similar backbones to those described herein has been well-developed by Moore and co-workers,[15−17] and oligoarylacetylenes with a slightly different backbone have been built by Lutz and co-workers.[18] Although the synthesis of these hetero-oligomers represents an important synthetic milestone, these molecules did not contain the reactive groups necessary to form dynamic covalent bonds. The Moore group subsequently synthesized arylacetylene homo-oligomers containing either aniline or benzaldehyde functional groups and showed that when mixed, these condensed to form molecular ladders through imine bonds.[19] These homo-oligomers avoid the complications resulting from the simultaneous presence of coreactive functional groups within one molecule, but as a consequence, they do not store information. To our knowledge, no general method for the synthesis and isolation of arbitrary sequence-defined polymers bearing reversible covalent recognition units capable of information storage and reversible bond formation has been reported. Only single sequences[9] and sequences with protected recognition units have been described.[20] Recently, two heterotrimers bearing boronic acid and catechol recognition units were described by Ng and co-workers,[21] but the synthetic methods for the heteropolymer sequences were not fully described, and the dynamic behavior of the individual heteromeric sequences was not addressed.

Methods to control and reverse the many potential intramolecular and intermolecular base-pairing interactions of these dynamic molecules have not been well-developed. $Sc(OTf)_3$ has been reported to catalyze transimination reactions and to affect the equilibration and equilibrium of aniline and benzaldehyde condensation and hydrolysis.[22,23] However, this approach has only been shown to facilitate the formation of duplexes between homopolymers[20,24] and hetero-

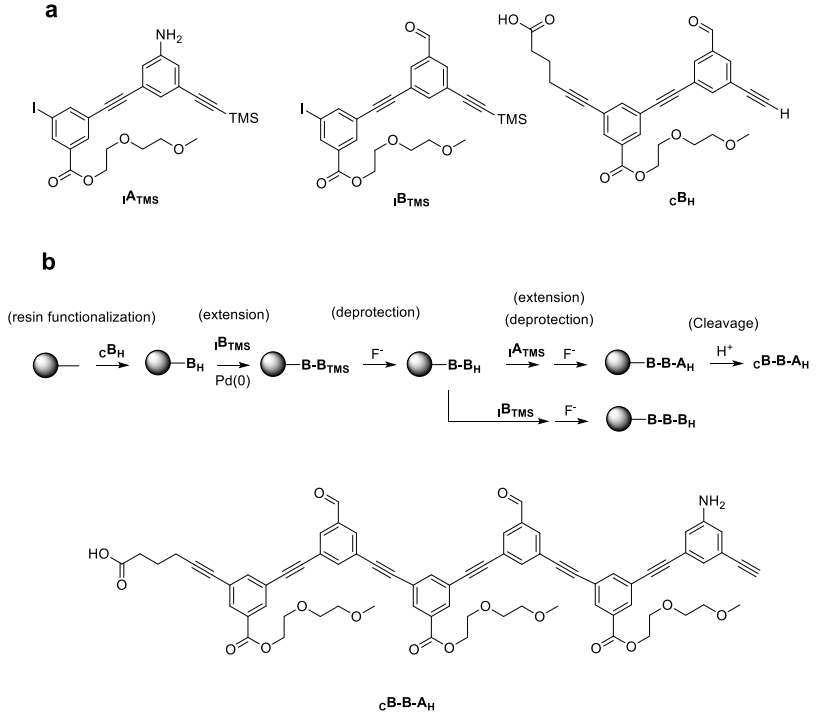

Figure 2. Solid-phase synthesis of sequence-defined ABOs.

https://dx.doi.org/10.1021/acs.joc.0c01977
J. Org. Chem. 2020, 85, 13929−13938

Scheme 1. Synthesis of Monomers $_{I}A_{TMS}$ and $_{I}B_{TMS}$

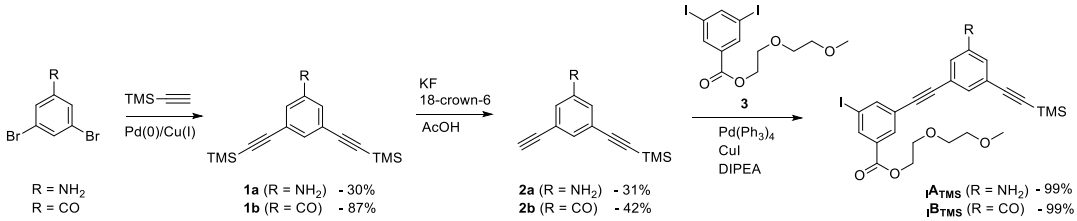

oligomers with masked recognition units.[19,25] For the hetero-oligomers, $Sc(OTf)_3$ was cleverly employed by Scott and co-workers to both catalyze the removal of acetal-protecting groups from benzaldehyde *in situ* and to facilitate imine formation. The single-stranded oligomers containing both aniline and benzaldehyde functional groups could not be isolated as such but were inferred from duplexes formed between complementary sequences. They assert that their strategy of protection of at least one reactive group and *in situ* deprotection is inherently necessary for the synthesis and handling of oligomers containing multiple coreactive groups capable of forming dynamic covalent bonds. Compared to genetic biopolymers, which are routinely manipulated as single strands without chemical modifications, the uncontrolled formation of intra- and intermolecular imine base pairs would pose a significant limitation. The effects of temperature, pH, metal ions, and ionic strength are comparatively well-understood for biopolymers so that they can be predictably interconverted between their folded, single-stranded, and double-stranded states.[26−28] Understanding how to manipulate synthetic aniline benzaldehyde oligoarylacetylenes (ABOs) in their native unmodified state is critical for an exploration of the folding and replication of such oligomers, and we have therefore explored protecting group-free methods for the synthesis, purification, and characterization of such hetero-oligomers. Herein, we describe an efficient means of constructing sequence-defined ABOs on solid supports. We then discuss how these molecules can be maintained as kinetically stable single-stranded oligomers or returned to their single-stranded state following common manipulations such as concentration which are apt to generate intractable mixtures of higher-order structures.

RESULTS AND DISCUSSION

Solid-Phase Synthesis of ABOs. In order to study the informational properties of aniline benzaldehyde oligoarylacetylenes, we developed a method for the solid-phase synthesis of sequence-defined ABOs. Our synthetic strategy relied on access to two monomers functionalized with an aryl iodide on one side and a TMS-protected alkyne on the other, $_{I}A_{TMS}$ and $_{I}B_{TMS}$, and the carboxylic acid-functionalized monomer $_{C}B_{H}$ (Figure 2a). We imagined that $_{C}B_{H}$ could be easily attached to a chlorotrityl-functionalized polystyrene solid support and then oligomers of any desired sequence could be built through iterative rounds of chain extension *via* Pd(0)-catalyzed Sonogashira coupling[29] and fluoride-mediated TMS deprotection (Figure 2b).[30] Once the desired sequence was constructed, acid-catalyzed cleavage from the resin would afford the desired sequence-defined oligomers.

The synthesis of the appropriately functionalized monomers $_{I}A_{TMS}$ and $_{I}B_{TMS}$ is depicted in Scheme 1. Starting from commercially available 2,5-dibromoaniline and 2,5-dibromobenzaldehyde, a double Sonogashira coupling with TMS-acetylene gave compounds **1a** and **1b** in acceptable yields. Breaking the symmetry of these molecules proved somewhat difficult. Standard methods using TBAF or K_2CO_3 gave complete deprotection of both alkynes, whereas more mild fluoride sources such as HF·Pyridine or TEA·3HF gave no detectible reaction even after heating at 50 °C overnight. We then considered that a single equivalent of a moderately available fluoride and a mild proton source would be ideal to maximize the yield of the singly deprotected product. A mixture of KF (1 equiv), a small amount of 18-crown-6 (0.25 equiv), and acetic acid (2 equiv) in THF gave clean conversion to the expected stoichiometric product distribution, approximately, 25% unreacted starting materials **1a** and **1b**, 50% of the desired singly deprotected products **2a** and **2b**, and 25% of the doubly deprotected diacetylenes, as assessed by LCMS (Figures S2 and S3). The desired products could be isolated in 31% (**2a**) and 42% (**2b**) yields, the unreacted starting materials recovered in 18% (**1a**) and 24% (**1b**) yields, and the doubly deprotected diacetylenes isolated in 13 and 12% yield. The monoprotected diynes **2** were then coupled to diiodide **3** using standard Sonogashira coupling conditions. In order to disfavor double coupling to the diiodides, the use of 10 equiv of **3** was necessary. This excess could be recovered nearly quantitatively and reused. The desired monomers $_{I}A_{TMS}$ and $_{I}B_{TMS}$ were obtained in excellent yields, and none of the double coupling product was observed. The initial monomer for solid-phase synthesis $_{C}B_{H}$ was functionalized with a carboxylic acid for attachment to the resin bead. Sonogashira coupling of $_{I}B_{TMS}$ with 5-hexynoic acid, followed by TMS deprotection with TBAF gave $_{C}B_{H}$ in acceptable yield (38% over two steps, Scheme S1).

Following the scheme outlined in Figure 2, $_{C}B_{H}$ was attached to chlorotrityl-functionalized polystyrene beads under mildly basic conditions. To make handling of the resin-bound material easier and to avoid site−site interactions, resin loading was reduced by a factor of 10 during the addition of the first monomer by the addition of a 10-fold excess of acetic acid relative to $_{C}B_{H}$. Coupling steps were accomplished in toluene under copper-free Sonogashira coupling conditions using the $AsPh_3$ ligand, $Pd_2(dba)_3$ as a catalyst, and DIPEA as a base.[31] With an excess of monomers $_{I}A_{TMS}$ or $_{I}B_{TMS}$ (6 equiv), coupling was completed cleanly in 1−3 h at 50 °C. After coupling, the unreacted monomer could be recovered from the organic solvent used to wash the resin beads and reused in subsequent couplings after repurification. Under the Sonogashira coupling conditions, no imine bonds between reacting monomers and complementary sites on the growing oligomer were observed. TMS deprotection was accomplished in 10 min at 25 °C using TBAF (20 mM) buffered with AcOH (20 mM) and stabilized with BHT (20 mM) in degassed THF.

Following the protocol described above, we synthesized a set of eight oligomers ranging in length from dimers to tetramers

https://dx.doi.org/10.1021/acs.joc.0c01977
J. Org. Chem. 2020, 85, 13929−13938

(Table 1). The yields presented in Table 1 are isolated yields following a short normal-phase silica column. LCMS

Table 1. Isolated Yields of Synthesized ABOs

entry	sequence	yield (%)
1	$_{C}BB_{H}$	90
2	$_{C}BA_{H}$	71
3	$_{C}BBB_{H}$	83
4	$_{C}BBA_{H}$	68
5	$_{C}BAA_{H}$	59
6	$_{C}BAB_{H}$	66
7	$_{C}BBBA_{H}$	37
8	$_{C}BABB_{H}$	56

chromatograms of the syntheses are shown in Figure S1. For the homo-oligomers $_{C}\mathbf{BB}_{H}$ and $_{C}\mathbf{BBB}_{H}$, purification and characterization required no special handling; however, for hetero-oligomers, special care needed to be taken to prevent imine base-pairing between **B** and **A** subunits, which could lead to the formation of dynamic mixtures. Our efforts to understand and control these dynamic equilibria are presented in the next section, as well as our strategy to isolate and characterize the hetero-oligomers.

In addition to furnishing sequence-defined oligomers, our method differs from the impressive solid-phase synthesis of similar aniline benzaldehyde *m*-phenylene ethynylene homopolymers reported by Moore and co-workers[19] in a few noteworthy details. For our approach, protecting groups on the aniline or benzaldehyde monomers were not required. In addition, we simplified the synthesis of the requisite monomers and used an air-stable palladium/ligand system requiring only that the head space of the reaction vessel be purged with inert gas prior to coupling. Finally, the addition of each monomer to the growing oligomer required only a single coupling and deprotection step, opposed to two.

Dynamic Behavior of ABOs. The equilibrium distribution of imine bonds and their hydrolyzed precursors is known to depend on many factors, such as the solvent, pH, temperature, available water for hydrolysis, available amines for transimination reactions, and presence of metal catalysts.[32−35] Disequilibrium states are also possible as the kinetics of imine bond formation can change drastically under different conditions, and populations can become kinetically trapped if imine formation or exchange is sufficiently slowed. Generally, under mildly acidic conditions, the rate of imine formation and hydrolysis is fast and favors the hydrolyzed amine and aldehyde products, while under more basic conditions, imine formation and hydrolysis is slower but imine formation is favored at equilibrium.

As illustrated in Figure S1, LCMS analysis of the crude products suggested that the solid-phase synthesis had been quite successful. However, for even the simplest heteromeric dimer $_{C}\mathbf{BA}_{H}$, ^{1}H NMR spectroscopy of the product following cleavage from the resin with TFA showed uninterpretable broad resonances (Figure 3a). Only after the addition of a small amount of H_2O or D_2O (3−10 μL to a sample in 600 μL of $CDCl_3$) did the expected spectrum of the single-stranded $_{C}\mathbf{BA}_{H}$ appear (Figure 3b). Surprisingly, when TEA was added instead of water, an entirely different spectrum was observed, which was confirmed by HRMS[36] to be the self-complementary duplex, ds-$_{C}\mathbf{BA}_{H}$ (Figure 3c). The single- and double-

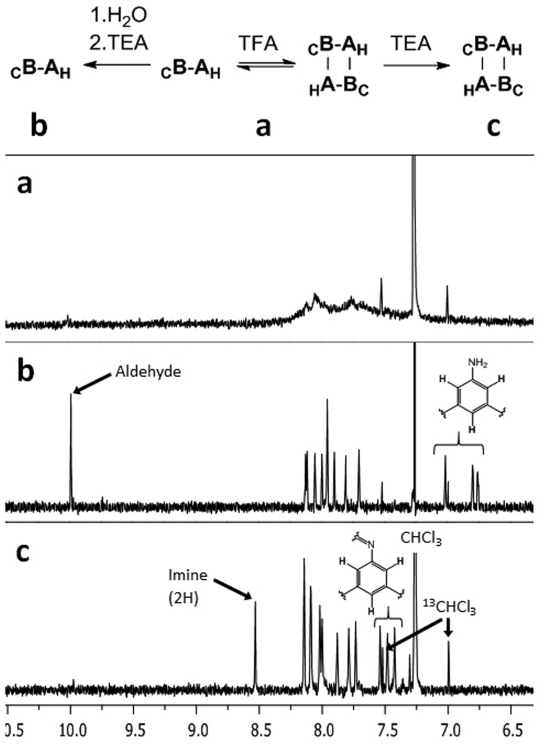

Figure 3. Dynamic behavior of $_{C}BA_{H}$. Equilibrium between single-stranded and duplex structure (top). (a) ^{1}H NMR spectrum of crude $_{C}\mathbf{BA}_{H}$ (2 mM) in $CDCl_3$ with 2% TFA (v/v). (b) Solution from **a** after 5 μL of D_2O was added and then 30 μL of TEA was added. (c) Solution from **a** after 30 μL of TEA was added.

stranded forms appeared to be quite stable, in that when TEA was added to the water-quenched solution, no change in the amount of ss-$_{C}\mathbf{BA}_{H}$ was observed in the NMR spectrum after two days and similarly, when water was added to the TEA-quenched solution, no change in the amount of ds-$_{C}\mathbf{BA}_{H}$ was observed in the NMR spectrum after two days. However, when the excess TEA was removed from the solution of ds-$_{C}\mathbf{BA}_{H}$ *in vacuo* and the dimer was redissolved in $CDCl_3$ with TFA and H_2O, the NMR spectrum showed complete conversion to ss-$_{C}\mathbf{BA}_{H}$.

The simplest explanation for these results is that the acidic and relatively anhydrous environment of the resin cleavage conditions favored the fast exchange of imine bonds on the time scale of the NMR such that only broad peaks corresponding to the time average of many different equilibrating species and their various protonation states were observed. Adding water to these acidic solutions likely shifted the equilibrium nearly entirely to hydrolysis of the imine bonds and the spectrum of ss-$_{C}\mathbf{BA}_{H}$ emerged. Adding TEA sequestered the acidic protons and prevented imine exchange reactions such that the spectrum of the thermodynamically favored ds-$_{C}\mathbf{BA}_{H}$ emerged. Once formed, solutions of ss-$_{C}\mathbf{BA}_{H}$ and ds-$_{C}\mathbf{BA}_{H}$ did not interconvert under identical conditions with added water and TEA, strongly suggesting that in the absence of a proton source, these solutions were kinetically stable. This insight proved vital for handling and purifying both these heterodimers and the longer hetero-oligomers. Basified solutions of such oligomers were therefore purified by chromatography on base-treated silica gel using THF with a 0−20% water gradient. Attempts to purify hetero-oligomers without quenching the acid with TEA failed

https://dx.doi.org/10.1021/acs.joc.0c01977
J. Org. Chem. 2020, 85, 13929−13938

presumably because dynamic mixtures were generated during washing or on the column.

The formation of duplexes between fully self-complementary dimers was expected, based on our previous work,[8] other work with longer homopolymeric ABOs,[19] and recent work with structurally similar aniline- and benzaldehyde-functionalized peptoids.[20] However, we expected the behavior of the heteropolymer trimers synthesized here to be more complex than simple duplex formation as these sequences are only partially self-complementary. They could potentially form several different self-complementary duplexes, higher-order oligomers, or folded structures. For example, a duplex ds-$_{C}$**BBA**$_{H}$ formed from the sequence $_{C}$**BBA**$_{H}$ would leave sticky ends of unpaired monomers, while out of register base pairing could create poly-$_{C}$**BBA**$_{H}$ and intramolecular base-pairing could potentially create a macrocyclic folded structure (Scheme 2).

Scheme 2. Potential Dynamic Behavior of $_{C}$BBA$_{H}$

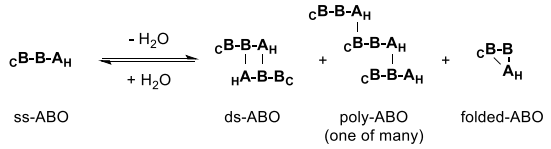

We searched for conditions that would allow us to effectively control the equilibria of the more complicated trimer and tetramer sequences so that we could routinely handle and characterize such molecules. Analogous to our observations of $_{C}$**BA**$_{H}$, the crude ^{1}H NMR spectra of the heteromeric trimers and tetramers under the acidic resin cleavage conditions ($CDCl_3$ with 2% TFA v/v) gave only broad resonances (*e.g.*, $_{C}$**BBA**$_{H}$, Figure 4a). Only after the addition of a small amount of D_2O (3−10 μL) did the expected spectrum of the single-stranded trimer appear (Figure 4b). Unlike the $_{C}$**BA**$_{H}$ sequence, these equilibria were found to be quite sensitive to the ratio of TFA to D_2O, and adding more than a few microliters of H_2O or D_2O to samples in 500 μL of $CDCl_3$ led

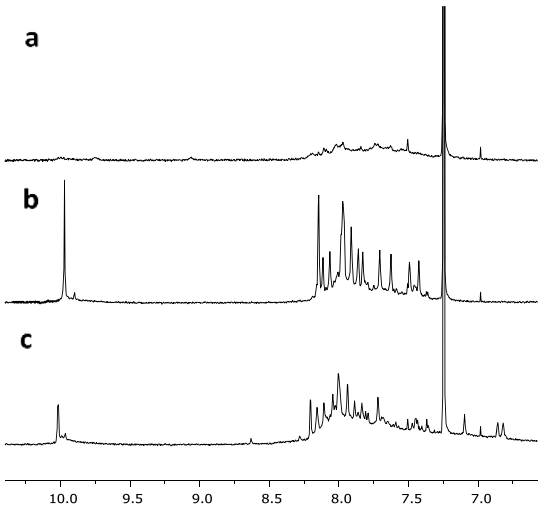

Figure 4. ^{1}H NMR spectra of the heterotrimer $_{C}$**BBA**$_{H}$. (a) Crude $_{C}$**BBA**$_{H}$ (approx. 5 mM) in 600 μL of $CDCl_3$ with 2% (v/v) TFA. (b) Solution from **a** immediately after 5 μL of D_2O was added. (c) Solution from **b** immediately after 200 μL of D_2O was added.

to the appearance of several new sets of peaks, including small peaks consistent with an imine functional group (*e.g.*, $_{C}$**BBA**$_{H}$ Figure 4c, δ 8.61 ppm).

To better understand the effect of added water on these systems, we compared the area of the two aldehyde ^{1}H NMR resonances of ss-$_{C}$**BBA**$_{H}$ (δ 10.05 ppm) and the peak area of the presumed imine proton resonance (δ 8.61 ppm) as D_2O was added to a 5 mM solution of $_{C}$**BBA**$_{H}$ in 500 μL of $CDCl_3$ with 2% TFA (v/v) (Figure 5).[37] Only in a narrow range of

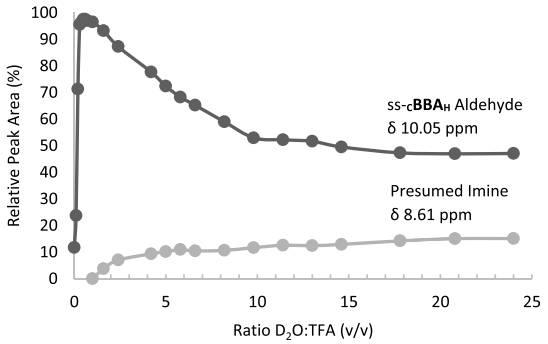

Figure 5. ^{1}H NMR signal of $_{C}$**BBA**$_{H}$ in $CDCl_3$ with 2% TFA (v/v) and added D_2O.

conditions were solutions found to be well-behaved and to give sharp peaks consistent with the expected spectrum of ss-$_{C}$**BBA**$_{H}$. With a ratio of 1:2 D_2O to TFA, the spectra showed only ss-$_{C}$**BBA**$_{H}$.

This trend was observed for all heteromeric-ABOs shown in Table 1. Hetero-oligomers were thus characterized by ^{1}H NMR under conditions which assured the predominately single-stranded state [$CDCl_3$ with 5% TFA and 1% H_2O (v/v)]. Heating the samples to 50 °C moved the H_2O/TFA resonance upfield so as to not overlap with the analyte peaks. At oligomer concentrations above 10 mM, significant peak broadening was observed by ^{1}H NMR which could not be completely reduced by adjusting the ratio of TFA and H_2O. Such higher concentrations may favor the intermolecular formation of imine bonds which cannot be entirely overcome. For homopolymeric-ABOs ($_{C}$**BB**$_{H}$ and $_{C}$**BBB**$_{H}$), no dynamic behavior was observed as expected because these molecules lack the anilines necessary for imine formation. We are currently working to fully describe the dynamic behavior of the trimers and tetramers we have synthesized under conditions which favor imine bonds.

Understanding the sensitivity of ABOs to the ratio of TFA and water in a solvent was vital for effective handling. For example, when pure ss-$_{C}$**BBA**$_{H}$ in $CDCl_3$ was concentrated to dryness, up to 30% of the starting mass was lost as insoluble white solids, and the material that was resolubilized was found by ^{1}H NMR to be about 60% ss-$_{C}$**BBA**$_{H}$ and 40% complex heterogeneous materials. We have previously reported that wet/dry cycles of aniline- and benzaldehyde-containing solutions are effective at forming imine bonds,[8] so we suspected that the hetero-oligomers were forming higher-order structures through condensation of **B** and **A** subunits, with some of these structures being insoluble in $CDCl_3$. We were initially unable to recover these insoluble products as they were insoluble in all pure solvents tested as well as with various mixtures of solvents along with the added acid and water expected to favor imine hydrolysis. Only with the precise ratio of TFA and water corresponding to the peak in Figure 5 (5:1

https://dx.doi.org/10.1021/acs.joc.0c01977
J. Org. Chem. 2020, 85, 13929−13938

TFA/H_2O v/v) were the materials resolubilized and the mixture of products observed in the ^1H NMR resolved to ss-$_C$**BBA**$_H$. These conditions proved very robust, and $CHCl_3$ with 5% TFA and 1% H_2O (v/v) was used routinely to return hetero-ABOs to their single-stranded form following purification and concentration.

CONCLUSIONS

The "holy grail" of Orgel[38] and many subsequent polymer chemists has been the synthesis of sequence-defined polymers with the ability to undergo Darwinian evolution, but with all the diversity in structure that chemistry and creativity will allow. Realizing this ambitious goal requires ready access to sequence-defined polymers with reversible recognition between subunits. Chemical methods for the synthesis, purification, concentration, annealing, denaturation, and folding of RNA and DNA have been fine-tuned by chemists and biochemists for the better part of a century.[39,40] Our understanding of how to manipulate these and closely related polymers and to control their dynamic behaviors is accordingly quite well-developed. For synthetic oligomers very different in structure from nucleotide-based oligomers, developing conditions to control their dynamic behavior is an integral part of their synthesis. For oligomers with imine-based reversible covalent recognition units, precisely controlling the amount of TFA and water proved a straightforward and effective way to ensure that solutions of these molecules were in their fully hydrolyzed state. This allowed for single-stranded oligomers to be observed by ^1H NMR and ESI−MS, to be returned to solution following concentration, and to be purified without the dynamic behavior of their subunits generating mixtures. The solid-phase synthesis developed herein is concise and high yielding. We imagine that these synthetic efforts will provide a solid foundation on which to build oligomers of any desired sequence and a starting point to more fully describe their dynamic behavior. Our observations and methods may prove useful to other chemists using imine condensation and hydrolysis in dynamic covalent chemistry contexts.

EXPERIMENTAL SECTION

General. The ^1H NMR and ^{13}C NMR spectra were recorded at 93.94 kG (^1H 400 MHz, ^{13}C 100 MHz) at ambient temperature or 50 °C, as noted. Hydrogen chemical shifts are expressed in parts per million (ppm) relative to the residual protio-solvent resonance: $CDCl_3$: δ 7.26. For ^{13}C spectra, the centerline of the solvent signal was used as the internal reference: $CDCl_3$: δ 77.00. Unless otherwise noted, each carbon resonance represents a single carbon (relative intensity). LCMS spectra were obtained on an Agilent Technologies system HPLC with a phenyl hexyl reverse-phase column. Mobile phases were water with 0.1% formic acid and THF using a THF gradient from 55 to 75%. Mass-to-charge ratios were determined from an inline electrospray (ESI) source in the positive ion mode and a Thermo Scientific quadrupolar mass analyzer. The MS settings were a capillary voltage of 3.5 kV and a desolvation temperature of 325 °C. High-resolution mass spectrometric data were obtained on a ToF (time-of-flight) Agilent Technologies system by electrospray (ESI) in the positive ion mode. Samples were injected as 10 μM solutions in 8:2 THF/H_2O. The MS settings were a capillary voltage of 4000 V, a desolvation temperature of 300 °C, and a fragmentor voltage of 500 V.

Solid-Phase Synthesis, Attachment of the First Monomer, $_C$B$_H$. Polystyrene resin beads (0.5−2 g) functionalized with 2-chlorotrityl chloride (1% DVB, 1.3 mmol/g loading) were added to a 40 mL scintillation vial. Anhydrous DCE (5 mL/g resin) was added and the resin allowed to swell for 5 min. To a separate vial, $_C$**B**$_H$ (0.22 equiv, 135 mg/g resin, 0.29 mmol/g resin) was added and dissolved in DCE (5 mL/g resin) and DIPEA (1.4 mL/g resin). Acetic acid (1.5 equiv, 114 μL/g resin, 2 mmol/g resin) was added to the $_C$**B**$_H$ solution and then this mixture was added to the vial containing the swelled resin beads. After the beads were shaken gently overnight, they were transferred to a sintered glass washing vessel using DCM and washed with 5 portions of DCM (50 mL/g resin). The washed beads were then transferred to a storage vial and dried under high vacuum (approx. 0.2 mbar) for several hours to remove the residual solvent. The resin loading was determined by quantitative ^1H NMR as follows: An aliquot (10.0 mg) of dry resin was added to an NMR tube and swelled in $CDCl_3$ (600 μL). TFA (5 μL) was added and the ^1H NMR spectrum was recorded immediately. Cleavage was found to be complete after 5 min and NMR spectra recorded at subsequent times (10 min and 1 h) showed no change. To the NMR tube, 50 μL of a 2.0% solution of DMF in $CDCl_3$ was added and the ^1H spectrum with a d1 relaxation delay of 10 s and 45 deg pulse angle was acquired. The normalized area of the DMF standard was then used to calculate the quantity of $_C$**B**$_H$ from which the resin loading could also be calculated. The resin loading was found to be 90−115 μmol/g $_C$**B**$_H$ and around 1.2 mmol/g acetic acid, which is in accordance with the commercially reported 1.3 g/mol loading of the beads.

Solid-Phase Synthesis, Extension of the Chain *via* Sonogashira Cross Coupling. To a 20 mL scintillation vial, $AsPh_3$ (8 mol/10 mol resin load) and $Pd_2(dba)_3$ (1 mol/10 mol resin load) were added and dissolved in anhydrous toluene (1 mL/5 μmol $Pd_2(dba)_3$). The head space of the vial was purged with argon and then the vial was sealed with a screw on cap. The purple solution was gently swirled until the $Pd_2(dba)_3$ dissolved and the color changed to bright yellow (approx. 10 min). To a separate 40 mL vial equipped with a stir bar, the resin (100 mg to 2 g, with a loading from 90 to 115 μmol/g) to be extended was added and swelled in toluene (5 mL/g resin) and DIPEA (2 mL/g resin). To this solution, the desired TMS-protected monomer $_I$**A**$_{TMS}$ or $_I$**B**$_{TMS}$ (6 equiv) was added and stirred gently to dissolve (approx. 5 min). Once the monomer had dissolved, the catalyst solution was added through a small cotton filter to the vial containing the resin. The head space of the reaction vessel was purged with argon and then the vial was sealed with a screw on cap. The reaction mixture was heated in an oil bath to 50 °C and stirred very gently for 3 h or until LCMS analysis of an aliquot of the reaction showed extension to be complete. The reaction mixture was allowed to cool to room temperature and then transferred to a sintered glass washing vessel using DCM and washed with 5 portions of DCM (50 mL/g resin). The DCM washes were combined and the unreacted monomers could be recovered and reused following a normal-phase flash column. The washed beads were transferred to a storage vial and dried under high vacuum (approx. 0.2 mbar) for several hours to remove the residual solvent. LCMS analysis of the resin beads was accomplished as follows: 10 mg of the resin was added to a 2 mL HPLC vial and swelled in 500 μL of DCM. To this, 30 μL of TFA was added, followed by 5 μL of H_2O. This solution was then diluted, 50 μL into 1 mL of 9:1 THF/H_2O, and the diluted solution was analyzed by LCMS as described in the General section (above).

Solid-Phase Synthesis, TBAF Cleavage of the TMS-Protecting Group. To a 20 mL scintillation vial, TBAF·3H_2O (0.4 mmol/g resin) was added and dissolved in dry degassed THF (10 mL/g resin) stabilized with 250 ppm BHT. To this solution, BHT (0.4 mmol/g resin) and AcOH (0.4 mmol/g resin) were added. The head space of the vial was purged with argon and then the vial was sealed with a screw on cap until ready for use. To a separate vial equipped with a stir bar, the resin to be deprotected was added (100 mg to 2 g, with a loading from 90 to 115 μmol/g) and swelled with dry degassed THF (10 mL/g resin) stabilized with 250 ppm BHT. The resin solution was stirred gently at 25 °C and the TBAF/BHT/AcOH solution was added in one portion. After stirring for 10 min, the reaction was quenched by adding ice (approx. 50 g/g resin). The reaction mixture was then transferred to a sintered glass washing vessel using stabilized THF and washed with 2 portions of THF (50 mL/g resin), then 2 portions of water (50 mL/g resin), and finally 5 portions of DCM (50 mL/g resin). The washed beads were transferred to a storage vial and

https://dx.doi.org/10.1021/acs.joc.0c01977
J. Org. Chem. 2020, 85, 13929−13938

dried under high vacuum (approx. 0.2 mbar) for several hours to remove the residual solvent. Success of the cleavage was verified by LCMS analysis following the same protocol outlined in the previous section.

Using THF free of residual peroxides was vital to the success of this reaction as compounds consistent with oxidation products were otherwise observed. Dissolving aldehyde-containing oligomers in THF with any detectable peroxides was detrimental, and detectable oxidation products were observed after sitting a few hours. Oxidation was greatly exacerbated by concentrating the material *in vacuo*, giving products consistent with multiple oxidation events corresponding to the number of aldehyde functional groups (Figure S4). We suggest that peroxy radicals generated from exposure of THF to air initiated auto-oxidation of the aldehyde functional groups to carboxylic acids.[41] No oxidation side products were observed when using freshly distilled THF or THF stabilized with 250 ppm BHT and stored under an inert atmosphere. No oxidation was observed in air for non-THF solvents.

Solid-Phase Synthesis, Cleavage from the Resin Beads and Purification. The resin (20−100 mg) was added to a resin-washing vessel and treated for 5 min with $CDCl_3$ or DCM with 0.5% TFA and 0.1% H_2O (10 mL/g resin). The organic solution was collected by filtration and the procedure was repeated three more times. The resin was then washed with a single portion of $CDCl_3$ or DCM (10 mL/g). To the combined organic washes, TEA (20 mL/g) was then added in a single portion and the solution was allowed to stand for 10 min. The organic solution was then washed with three portions of water (25 mL/g) and one portion of brine (25 mL/g). The aqueous washes were discarded and the organic phase was loaded directly onto a short normal-phase silica gel column which had been packed with DCM containing 0.5% TEA. The column was run with freshly distilled THF buffered with 0.1% TEA and a water gradient from 0 to 20% over 30 min with a flow rate of 2 mL/min. The fractions containing the desired products were concentrated to a white solid on a speedvac rotary concentrator. The pure materials were dissolved in DCM or $CDCl_3$ for NMR, LCMS, or HRMS analysis. For heteropolymers, 0.5% TFA and 0.1% H_2O were added to the solvent. Following analysis, the TFA could be removed by washing the organic phase with several portions of water and then the materials could be concentrated to a white powder for storage.

*3,5-Bis((trimethylsilyl)ethynyl)aniline (**1a**).* To a 200 mL round-bottom flask equipped with a stir bar, 3,5-dibromoaniline (1.0 g, 4 mmol) was added and then dissolved in anhydrous toluene (20 mL) and DIPEA (10 equiv, 20 mmol, 7 mL). The solution was sparged with argon for 30 min and then TMS-acetylene (4 equiv, 16 mmol, 2.32 mL) was added, followed by $Pd(PPh_3)_4$ (0.02 equiv, 0.08 mmol, 92 mg) and CuI (0.05 equiv, 0.2 mmol, 36 mg). The head space of the reaction vessel was purged with argon and the flask was sealed with a glass stopper. After stirring overnight at 55 °C, the reaction mixture was cooled to room temperature and diluted with DCM (approx. 100 mL), and dry silica (approx. 10 g) was added. The mixture was then concentrated onto the silica gel using rotoevaporation and the resulting white powder was used to dry load a silica gel column. Normal-phase silica gel flash chromatography (80 g silica column, hexane with a 5−50% gradient of EtOAc over 25 min) gave a 1:1 mixture of doubly alkynylated product **1a** and singly alkynylated side product 3-bromo-5-((trimethylsilyl)ethynyl)aniline. The mixture of products was concentrated to a light yellow oil and then subjected to a C18 reverse-phase flash column (50 g column loaded using 5 mL DMF, then run with water and a 45−95% ACN gradient over 15 min). The reverse-phase column afforded pure **1a** (eluted from 85 to 90% ACN, 340 mg, 1.19 mmol, 30% yield) as a colorless oil. ^{1}H NMR (400 MHz, $CDCl_3$): δ 7.00 (t, J = 1.4 Hz, 1H), 6.71 (d, J = 1.4 Hz, 2H), 3.64 (s, 2H), 0.22 (s, 18H); $^{13}C\{^1H\}$ NMR (100 MHz, $CDCl_3$): δ 146.0, 126.1, 123.9 (2C), 118.3 (2C), 104.4 (2C), 94.1 (2C), −0.1 (6C). HRMS (ESI) m/z: $[M + H]^+$ calcd for $C_{16}H_{24}NSi_2$, 286.1442; found, 286.1448.

*3,5-Bis((trimethylsilyl)ethynyl)benzaldehyde (**1b**).* To a 200 mL round-bottom flask equipped with a stir bar, 3,5-dibromobenzaldehyde (2.1 g, 8 mmol) was added and then dissolved in anhydrous toluene (40 mL) and DIPEA (10 equiv, 40 mmol, 14 mL). The solution was sparged with argon for 30 min and then TMS-acetylene (4 equiv, 32 mmol, 4.64 mL) was added, followed by $Pd(PPh_3)_4$ (0.02 equiv, 0.16 mmol, 184 mg) and CuI (0.05 equiv, 0.4 mmol, 72 mg). The head space of the reaction vessel was purged with argon and the flask was sealed with a glass stopper. After stirring overnight at 50 °C, the reaction mixture was cooled to room temperature and diluted with DCM (approx. 100 mL), and dry silica (approx. 10 g) was added. The mixture was then concentrated onto the silica gel using rotoevaporation and the resulting white powder was used to dry load a silica gel column. Normal-phase silica gel flash chromatography (80 g silica column, hexane with a 0−10% gradient of EtOAc over 25 min) gave a mixture of doubly alkynylated product **1b** and singly alkynylated side product 3-bromo-5-((trimethylsilyl)ethynyl)-benzaldehyde. The mixture of products was concentrated to a light yellow oil and then subjected to a C18 reverse-phase flash column (50 g column loaded using 5 mL DMF, then run with water and a 30−100% ACN gradient over 15 min). The reverse-phase column afforded pure **1b** (R_f = 2 min 100% ACN, 2.07 g, 6.93 mmol, 87% yield) as a colorless oil. ^{1}H NMR (400 MHz, $CDCl_3$): δ 9.94 (s, 1H), 7.87 (d, J = 1.6 Hz, 2H), 7.79 (t, J = 1.6 Hz, 1H), 0.25 (s, 18H); $^{13}C\{^1H\}$ NMR (100 MHz, $CDCl_3$): δ 190.7, 140.3 (2C), 136.4, 132.4 (2C), 124.6, 102.5 (2C), 97.0 (2C), −0.2 (6C). HRMS (ESI) m/z: $[M + Na]^+$ calcd for $C_{17}H_{22}OSi_2Na$, 321.1101; found, 321.1126.

*3-Ethynyl-5-((trimethylsilyl)ethynyl)aniline (**2a**).* To a 40 mL scintillation vial equipped with a stir bar, **1a** (330 mg, 1.16 mmol) was added and then dissolved in dry degassed THF stabilized with 250 ppm BHT (5.8 mL). To this solution, 18-crown-6 (76.4 mg, 0.25 equiv, 0.29 mmol), AcOH (2 equiv, 2.31 mmol, 132.4 μL), and KF (1.0 equiv, 1.16 mmol, 67 mg) were added. After stirring at room temperature overnight, the reaction was quenched by the addition of silica (approx. 2 g). The mixture was then concentrated onto the silica gel using rotoevaporation and the resulting white powder was used to dry load a silica gel column. Silica gel flash chromatography (40 g silica column, hexane with a 10−50% gradient of EtOAc over 18 min) gave the pure product (76 mg, 0.356 mmol, 31% yield) as a white solid. Starting material **1a** and doubly deprotected 3,5-diethynylanilne were also isolated in 18% and 13% yields, respectively. ^{1}H NMR (400 MHz, $CDCl_3$): δ 7.01 (t, J = 1.4 Hz, 1H), 6.78−6.72 (m, 2H), 3.67 (s, 2H), 3.00 (s, 1H), 0.23 (s, 9H); $^{13}C\{^1H\}$ NMR (100 MHz, chloroform-d): δ 146.1, 125.8, 123.9, 122.9, 118.5, 118.4, 104.3, 94.2, 83.0, 77.0, −0.2 (3C). HRMS (ESI) m/z: $[M + H]^+$ calcd for $C_{13}H_{16}NSi$, 214.1047; found, 214.1031.

*3-Ethynyl-5-((trimethylsilyl)ethynyl)benzaldehyde (**2b**).* To a 40 mL scintillation vial equipped with a stir bar, **1b** (313 mg, 1.05 mmol) was added and then dissolved in dry degassed THF stabilized with 250 ppm BHT (5.6 mL). To this solution, 18-crown-6 (69.3 mg, 0.25 equiv, 0.26 mmol), AcOH (2 equiv, 2.1 mmol, 120 μL), and KF (1.0 equiv, 1.05 mmol, 61 mg) were added. After stirring at room temperature overnight, the reaction was quenched by the addition of silica (approx. 2 g). The mixture was then concentrated onto the silica gel using rotoevaporation and the resulting white powder was used to dry load a silica gel column. Silica gel flash chromatography (40 g silica column, hexane with a 0−10% gradient of EtOAc over 18 min) gave a mixture of product **2b**, starting material **1b**, and doubly deprotected product 3,5-diethynylbenzaldehyde. Reverse-phase CombiFlash chromatography (50 g C18 column, water with 30% ACN increasing to 100% ACN over 20 min) gave pure **2b** as a white solid (99.8 mg, 0.44 mmol, 42% yield). Starting material **1b** and doubly deprotected 3,5-diethynylbenzaldehyde were also isolated in 24% and 12% yields, respectively. ^{1}H NMR (400 MHz, $CDCl_3$): δ 9.95 (s, 1H), 7.92 (t, J = 1.6 Hz, 1H), 7.90 (t, J = 1.6 Hz, 1H), 7.80 (t, J = 1.6 Hz, 1H), 3.16 (s, 1H), 0.26 (s, 9H); $^{13}C\{^1H\}$ NMR (100 MHz, $CDCl_3$): δ 190.3, 140.2, 136.4, 132.7, 132.4, 124.6, 123.5, 102.2, 97.2, 81.3, 79.4, −0.3 (3C). HRMS (ESI) m/z: $[M + Na]^+$ calcd for $C_{14}H_{14}OSiNa$, 249.0706; found, 249.0697.

*2-(2-Methoxyethoxy)ethyl 3-((3-amino-5-((trimethylsilyl)-ethynyl)phenyl)ethynyl)-5-iodobenzoate ($_I$**A_{TMS}**).* To a 200 mL round-bottom flask equipped with a stir bar, **2a** (111 mg, 0.52 mmol) was added and then dissolved in anhydrous toluene (5.2 mL) and DIPEA (3 equiv, 1.56 mmol, 271 μL). Diiodide **3** was added (10

equiv, 5.2 mmol, 2.48 g) and the solution was stirred until homogeneous (approx. 15 min). To the stirred solution, $Pd(PPh_3)_4$ (0.05 equiv, 0.026 mmol, 30 mg) and CuI (0.1 equiv, 0.052 mmol, 9.9 mg) were then added. The head space of the reaction vessel was purged with argon and the flask was sealed with a glass stopper. After stirring for 5 h at room temperature, dry silica was added. The mixture was then concentrated onto the silica gel using rotoevaporation and the resulting white powder was used to dry load a silica gel column. Normal-phase silica gel flash chromatography (40 g silica column, hexane with a 10−50% gradient of EtOAc over 18 min) gave a mixture of product $_{I}\mathbf{A}_{TMS}$ and **3**. The mixture of the product and reactant was concentrated to a light yellow oil and then subjected to a C18 reverse-phase flash column (50 g column loaded using 5 mL DMF, then run with water and a 50−100% ACN gradient over 5 min, followed by 100% ACN for 10 min). The reverse-phase column afforded pure **3** (eluted from 85 to 90% ACN, 4.63 mmol, 2.21 g, 99% recovery) as a white solid and desired product $_{I}\mathbf{A}_{TMS}$ (R_f = 5 min with 100% ACN, 295 mg, 0.52 mmol, 99% yield) as a waxy solid. ^{1}H NMR (400 MHz, $CDCl_3$): δ 8.32 (s, 1H), 8.12 (s, 1H), 8.00 (s, 1H), 7.06 (s, 1H), 6.77 (s, 2H), 4.53−4.46 (m, 2H), 3.86−3.82 (m, 2H), 3.76−3.66 (overlap, 4H), 3.61−3.55 (m, 2H), 3.40 (s, 3H), 0.24 (s, 9H); ^{13}C{^{1}H} NMR (100 MHz, $CDCl_3$): δ 164.3, 146.3, 143.9, 137.9, 131.8, 131.7, 125.5, 125.3, 124.1, 123.1, 118.5, 117.8, 104.2, 94.3, 93.2, 91.0, 86.4, 71.8, 70.5, 69.0, 64.5, 59.0, −0.2 (3C). HRMS (ESI) m/z: $[M + Na]^+$ calcd for $C_{25}H_{28}INO_4SiNa$, 584.0724; found, 584.0746.

2-(2-Methoxyethoxy)ethyl 3-((3-formyl-5-((trimethylsilyl)-ethynyl)phenyl)ethynyl)-5-iodobenzoate ($_{I}\mathbf{B}_{TMS}$). To a 200 mL round-bottom flask equipped with a stir bar, **2b** (165 mg, 0.73 mmol) was added and then dissolved in anhydrous toluene (7.3 mL) and DIPEA (3 equiv 2.19 mmol, 384 μL). Diiodide **3** was added (10 equiv, 7.3 mmol, 3.49 g) and the solution was stirred until homogeneous (approx. 15 min). To the stirred solution, $Pd(PPh_3)_4$ (0.05 equiv, 0.037 mmol, 42 mg) and CuI (0.1 equiv, 0.073 mmol, 13.9 mg) were then added. The head space of the reaction vessel was purged with argon and the flask was sealed with a glass stopper. After stirring for 2.5 h at room temperature, dry silica was added. The mixture was then concentrated onto the silica gel using rotoevaporation and the resulting white powder was used to dry load a silica gel column. Normal-phase silica gel flash chromatography (40 g silica column, hexane with a 10−50% gradient of EtOAc over 18 min) gave a mixture of product $_{I}\mathbf{B}_{TMS}$ and **3**. The mixture of the product and reactant was concentrated to a light yellow oil and then subjected to a C18 reverse-phase flash column (50 g column loaded using 5 mL DMF, then run with water and a 50−100% ACN gradient over 5 min, followed by 100% ACN for 10 min). The reverse-phase column afforded pure **3** (eluted from 85 to 90% ACN, 6.24 mmol, 2.97 g, 95% recovery) as a white solid and desired product $_{I}\mathbf{B}_{TMS}$ (R_f = 5 min with 100% ACN, 418 mg, 0.73 mmol, 99% yield) as a waxy solid. ^{1}H NMR (400 MHz, $CDCl_3$): δ 9.98 (s, 1H), 8.37 (t, J = 1.6 Hz, 1H), 8.16 (t, J = 1.6 Hz, 1H), 8.05 (t, J = 1.6 Hz, 1H), 7.95 (t, J = 1.6 Hz, 1H), 7.93 (t, J = 1.6 Hz, 1H), 7.86 (t, J = 1.6 Hz, 1H), 4.53−4.48 (m, 2H), 3.88−3.82 (m, 2H), 3.73−3.68 (m, 2H), 3.61−3.56 (m, 2H), 3.40 (s, 3H), 0.27 (s, 9H); ^{13}C{^{1}H} NMR (100 MHz, $CDCl_3$): δ 190.2, 164.0, 143.8, 139.7, 138.4, 136.4, 132.6, 131.83, 131.80, 131.77, 124.7, 124.4, 123.7, 102.2, 97.2, 93.2, 89.0, 88.5, 71.7, 70.4, 68.9, 64.5, 58.9, −0.4 (3C). HRMS (ESI) m/z: $[M + Na]^+$ calcd for $C_{26}H_{27}IO_5SiNa$, 597.0565; found, 597.0582.

6-(3-((3-Formyl-5-((trimethylsilyl)ethynyl)phenyl)ethynyl)-5-((2-(2-methoxyethoxy) ethoxy)carbonyl)phenyl)hex-5-ynoic Acid ($_{C}\mathbf{B}_{TMS}$). To a 20 mL scintillation vial, $AsPh_3$ (0.12 mmol, 37.2 mg) and $Pd_2(dba)_3$ (0.015 mmol, 14 mg) were added and dissolved in anhydrous DCE (1 mL). The head space of the vial was purged with argon and then the vial was sealed with a screw on cap. The purple solution was gently swirled until the $Pd_2(dba)_3$ dissolved and the color changed to bright yellow (approx. 10 min). In a separate vial equipped with a stir bar, $_{I}\mathbf{B}_{TMS}$ (175 mg, 0.30 mmol) was dissolved in anhydrous DCE (1 mL). To this solution, DIPEA (1 mL) and 5-hexynoic acid (0.46 mmol, 50 μL) were added. While stirring, a portion of the catalyst solution was added dropwise (0.6 mL). The head space of the vial was purged with argon, and the vessel was sealed with a screw on cap. After stirring at room temperature overnight, the reaction mixture was transferred to a round-bottom flask and diluted with DCM (approx. 50 mL). Silica gel was added to the vessel and the crude reaction mixture was concentrated onto the silica gel. Silica gel flash chromatography (hexane with a 30−100% gradient of EtOAc, each with 0.5% AcOH) gave the pure product (75 mg, 0.13 mmol, 45%) as a colorless oil. ^{1}H NMR (400 MHz, $CDCl_3$): δ 9.94 (s, 1H), 8.06 (s, 1H), 8.01 (s, 1H), 7.91 (s, 1H), 7.88 (s, 1H), 7.82 (s, 1H), 7.67 (s, 1H), 4.51−4.43 (m, 2H), 3.86−3.78 (m, 2H), 3.71−3.64 (m, 2H), 3.59−3.52 (m, 2H), 3.36 (s, 3H), 2.54 (t, J = 7.3 Hz, 2H), 2.50 (t, J = 6.9 Hz, 2H), 1.92 (tt, J = 7.3, 6.9 Hz, 2H), 0.24 (s, 9H); ^{13}C{^{1}H} NMR (100 MHz, $CDCl_3$): δ 190.6, 178.4, 165.1, 139.9, 138.3, 136.5, 132.8, 132.5, 132.0, 131.8, 130.7, 124.8, 124.6, 124.1, 123.0, 102.3, 97.2, 90.8, 89.6, 88.2, 79.8, 71.8, 70.4, 69.1, 64.4, 59.0, 32.7, 23.3, 18.7, −0.3 (3C). HRMS (ESI) m/z: $[M + Na]^+$ calcd for $C_{32}H_{34}O_7SiNa$, 581.1966; found, 581.1982.

6-(3-((3-Ethynyl-5-formylphenyl)ethynyl)-5-((2-(2-methoxyethoxy)ethoxy)carbonyl)phenyl)hex-5-ynoic Acid ($_{C}\mathbf{B}_{H}$). To a 20 mL scintillation vial, TBAF·$3H_2O$ (0.28 mmol, 88 mg) was added and dissolved in dry degassed THF stabilized with 250 ppm BHT. To this solution, BHT (0.28 mmol, 62 mg) and AcOH (0.28 mmol, 16 μL) were added. In a separate vial equipped with a stir bar, $_{C}\mathbf{B}_{TMS}$ (75 mg, 0.13 mmol) was dissolved in dry degassed THF stabilized with 250 ppm BHT (2.8 mL). The TBAF solution was then added to the $_{C}\mathbf{B}_{TMS}$ solution. The head space was purged with argon and the mixture was stirred at room temperature. After 5 min, the reaction was quenched by adding ice (approx. 5 g). After stirring for 1 min, silica (approx. 1 g) was added and the reaction mixture was concentrated *in vacuo*. Silica gel flash chromatography (hexane with a 30−100% gradient of EtOAc, each with 0.5% AcOH) gave the pure product (53 mg, 0.11 mmol, 85% yield) as a colorless oil which solidified to a white amorphous solid on refrigeration overnight. ^{1}H NMR (400 MHz, $CDCl_3$): δ 9.99 (s, 1H), 8.11 (s, 1H), 8.06 (s, 1H), 7.99 (s, 1H), 7.95 (s, 1H), 7.87 (s, 1H), 7.71 (s, 1H), 4.54−4.46 (m, 2H), 3.89−3.82 (m, 2H), 3.74−3.68 (m, 2H), 3.62−3.56 (m, 2H), 3.40 (s, 3H), 3.20 (s, 1H), 2.58 (t, J = 7.2 Hz, 2H), 2.54 (t, J = 6.9 Hz, 2H), 1.96 (tt, J = 7.2, 6.9 Hz, 2H); ^{13}C{^{1}H} NMR (100 MHz, $CDCl_3$): δ 193.1, 181.1, 167.8, 142.7, 141.1, 139.3, 135.5, 135.3, 135.2, 134.5, 133.4, 127.3, 126.9, 126.5, 125.6, 93.5, 92.5, 90.8, 83.9, 82.5, 82.3, 74.5, 73.1, 71.8, 67.1, 61.7, 35.4, 26.0, 21.4. HRMS (ESI) m/z: [M + Na] calcd for $C_{29}H_{26}O_7Na$, 509.1571; found, 509.1605.

$_{C}BB_{H}$. The resin (100 mg with 95 μmol/g loading) functionalized with $_{C}\mathbf{BB}_{H}$ was cleaved and purified according to the procedure outlined above, and $_{C}\mathbf{BB}_{H}$ (7.4 mg, 8.6 μmol, 90% yield) was afforded as a white solid. ^{1}H NMR (400 MHz, $CDCl_3$): δ 10.03 (s, 1H), 10.01 (s, 1H), 8.26−8.17 (overlap, 2H), 8.13 (t, J = 1.6 Hz, 1H), 8.07 (t, J = 1.7 Hz, 1H), 8.04−7.99 (overlap, 3H), 7.97 (t, J = 1.6 Hz, 1H), 7.95 (t, J = 1.7 Hz, 1H), 7.91−7.87 (overlap, 2H), 7.74 (t, J = 1.7 Hz, 1H), 4.60−4.45 (overlap, 4H), 3.94−3.81 (overlap, 4H), 3.78−3.67 (overlap, 4H), 3.65−3.54 (overlap, 4H), 3.41 (s, 3H), 3.41 (s, 3H), 3.22 (s, 1H), 2.59 (t, J = 7.3 Hz, 2H), 2.55 (t, J = 7.0 Hz, 2H), 1.97 (tt, J = 7.3, 7.0 Hz, 2H). HRMS (ESI) m/z: $[M + Na]^+$ calcd for $C_{52}H_{44}O_{12}Na$, 883.2725; found, 883.2879.

$_{C}BA_{H}$. The resin (20 mg with 100 μmol/g resin loading) functionalized with $_{C}\mathbf{BA}_{H}$ was cleaved and purified according to the procedure outlined above, and $_{C}\mathbf{BA}_{H}$ (1.2 mg, 1.4 μmol, 71% yield) was afforded as a white solid. ^{1}H NMR (400 MHz, $CDCl_3$ with 0.5% TFA and 0.1% H_2O): δ 10.00 (s, 1H), 8.20 (s, 1H), 8.16 (s, 1H), 8.10 (s, 1H), 8.06−8.00 (overlap, 3H), 7.97 (s, 1H), 7.90 (s, 1H), 7.76 (s, 1H), 7.74 (s, 1H), 7.53 (s, 1H), 7.48 (s, 1H), 4.63−4.47 (overlap, 4H), 3.97−3.86 (overlap, 4H), 3.84−3.75 (overlap, 4H), 3.75−3.68 (overlap, 4H), 3.48 (s, 3H), 3.47 (s, 3H), 3.26 (s, 1H), 2.64 (t, J = 7.3 Hz, 2H), 2.55 (t, J = 6.8 Hz, 2H), 1.98 (tt, J = 7.3, 6.8 Hz, 2H). HRMS (ESI) m/z: [M + Na] calcd for $C_{51}H_{45}NO_{11}Na$, 870.2885; found, 870.2859.

$_{C}BBB_{H}$. The resin (100 mg with 88 μmol/g resin loading) functionalized with $_{C}\mathbf{BBB}_{H}$ was cleaved and purified according to the procedure outlined above, and $_{C}\mathbf{BBB}_{H}$ (9.0 mg, 7.3 μmol, 83%

https://dx.doi.org/10.1021/acs.joc.0c01977
J. Org. Chem. 2020, 85, 13929−13938

yield) was afforded as a white solid. ^{1}H NMR (400 MHz, $CDCl_3$): δ 10.05 (s, 1H), 10.04 (s, 1H), 10.01 (s, 1H), 8.25−8.19 (overlap, 4H), 8.13 (t, J = 1.5 Hz, 1H), 8.07 (t, J = 1.3 Hz, 1H), 8.05−7.99 (overlap, 5H), 7.98−7.94 (overlap, 3H), 7.91 (t, J = 1.4 Hz, 1H), 7.90−7.88 (overlap, 2H), 7.74 (t, J = 1.4 Hz, 1H), 4.58−4.48 (overlap, 6H), 3.93−3.83 (overlap, 6H), 3.76−3.68 (overlap, 6H), 3.64−3.57 (overlap, 6H), 3.42 (s, 3H), 3.41−3.40 (overlap, 6H), 3.22 (s, 1H), 2.59 (t, J = 7.3 Hz, 2H), 2.55 (t, J = 7.0 Hz, 2H), 1.97 (tt, J = 7.3, 7.0 Hz, 2H). HRMS (ESI) m/z: $[M + Na]^+$ calcd for $C_{75}H_{62}O_{17}Na$, 1257.3879; found, 1257.3888.

$_CBBA_H$. The resin (50 mg with 111 μmol/g resin loading) functionalized with **$_CBBA_H$** was cleaved and purified according to the procedure outlined above, and **$_CBBA_H$** (4.6 mg, 3.8 μmol, 68% yield) was afforded as a white solid. ^{1}H NMR (400 MHz, $CDCl_3$ with 0.5% TFA and 0.1% H_2O): δ 9.99 (s, 1H), 9.97 (s, 1H), 8.23−8.17 (overlap, 3H), 8.15 (s, 1H), 8.09 (s, 1H), 8.07−8.02 (overlap, 4H), 8.01 (s, 1H), 8.00 (s, 1H), 7.98 (s, 1H), 7.94 (s, 1H), 7.91 (s, 1H), 7.77 (s, 1H), 7.75 (s, 1H), 7.53 (s, 1H), 7.48 (s, 1H), 4.62−4.51 (overlap, 6H), 3.98−3.89 (overlap, 6H), 3.85−3.77 (overlap, 6H), 3.77−3.70 (overlap, 6H), 3.49−3.47 (overlap, 6H), 3.47 (s, 3H), 3.24 (s, 1H), 2.63 (t, J = 7.3 Hz, 2H), 2.54 (t, J = 6.9 Hz, 2H), 1.98 (tt, J = 7.3, 6.9 Hz, 2H). HRMS (ESI) m/z: $[M + Na]^+$ calcd for $C_{74}H_{63}NO_{16}Na$, 1244.4039; found, 1244.4162.

$_CBAA_H$. The resin (60 mg with 95 μmol/g resin loading) functionalized with **$_CBAA_H$** was cleaved and purified according to the procedure outlined above, and **$_CBAA_H$** (4.1 mg, 3.4 μmol, 59% yield) was afforded as a white solid. ^{1}H NMR (400 MHz, $CDCl_3$ with 0.5% TFA and 0.1% H_2O): δ 9.97 (s, 1H), 8.18 (t, J = 1.5 Hz, 1H), 8.16−8.12 (overlap, 3H), 8.08 (t, J = 1.6 Hz, 1H), 8.03−7.99 (overlap, 3H), 7.96 (t, J = 1.5 Hz, 1H), 7.90 (t, J = 1.5 Hz, 1H), 7.86 (t, J = 1.5 Hz, 1H), 7.79 (s, 1H), 7.76 (t, J = 1.5 Hz, 1H), 7.72 (s, 1H), 7.56−7.51 (overlap, 3H), 7.47 (s, 1H), 4.60−4.50 (overlap, 6H), 3.97−3.87 (overlap, 6H), 3.83−3.76 (overlap, 6H), 3.75−3.69 (overlap, 6H), 3.48−3.45 (overlap, 9H), 3.24 (s, 1H), 2.63 (t, J = 7.3 Hz, 2H), 2.54 (t, J = 6.9 Hz, 2H), 1.98 (tt, J = 7.3, 6.9 Hz, 2H). HRMS (ESI) m/z: $[M + Na]^+$ calcd for $C_{73}H_{64}N_2O_{15}Na$, 1231.4199; found, 1231.4198.

$_CBAB_H$. The resin (80 mg, 95 μmol/g loading) functionalized with **$_CBAB_H$** was cleaved and purified according to the procedure outlined above, and **$_CBAB_H$** (6.1 mg, 5.0 μmol, 66% yield) was afforded as a white solid. ^{1}H NMR (400 MHz, $CDCl_3$ with 0.5% TFA and 0.1% H_2O): δ 9.98 (s, 1H), 9.95 (s, 1H), 8.20 (t, J = 1.6 Hz, 1H), 8.19 (t, J = 1.6 Hz, 1H), 8.18−8.16 (overlap, 2H), 8.09 (t, J = 1.6 Hz, 1H), 8.06−8.00 (overlap, 4H), 8.00−7.96 (overlap, 2H), 7.94−7.91 (overlap, 2H), 7.91 (t, J = 1.4 Hz, 1H), 7.83 (t, J = 1.4 Hz, 1H), 7.77 (t, J = 1.5 Hz, 1H), 7.58−7.54 (overlap, 2H), 4.61−4.51 (overlap, 6H), 3.97−3.89 (overlap, 6H), 3.84−3.77 (overlap, 6H), 3.76−3.70 (overlap, 6H), 3.49−3.47 (overlap, 6H), 3.47 (s, 3H), 3.22 (s, 1H), 2.64 (t, J = 7.3 Hz, 2H), 2.55 (t, J = 6.9 Hz, 2H), 1.99 (tt, J = 7.3, 6.9 Hz, 2H). HRMS (ESI) m/z: $[M + Na]^+$ calcd for $C_{74}H_{63}NO_{16}Na$, 1244.4039; found, 1244.4133.

$_CBBBA_H$. The resin (62 mg, 81 μmol/g loading) functionalized with **$_CBBBA_H$** was cleaved and purified according to the procedure outlined above, and **$_CBBBA_H$** (2.9 mg, 1.8 μmol, 37% yield) was afforded as a white solid. ^{1}H NMR (400 MHz, $CDCl_3$ with 0.5% TFA and 0.1% H_2O): δ 10.00 (s, 1H), 9.99 (s, 1H), 9.98 (s, 1H), 8.22−8.18 (overlap, 5H), 8.15 (t, J = 1.6 Hz, 1H), 8.09 (t, J = 1.6 Hz, 1H), 8.08−7.99 (overlap, 9H), 7.97 (t, J = 1.5 Hz, 1H), 7.95 (t, J = 1.6 Hz, 1H), 7.94 (t, J = 1.6 Hz, 1H), 7.90 (t, J = 1.5 Hz, 1H), 7.76 (t, J = 1.6 Hz, 1H), 7.75 (s, 1H), 7.54 (s, 1H), 7.48 (s, 1H), 4.62−4.51 (overlap, 8H), 3.98−3.88 (overlap, 8H), 3.85−3.77 (overlap, 8H), 3.77−3.70 (overlap, 8H), 3.49−3.48 (overlap, 9H), 3.47 (s, 3H), 3.24 (s, 1H), 2.64 (t, J = 7.3 Hz, 2H), 2.55 (t, J = 6.8 Hz, 2H), 1.99 (tt, J = 7.3, 6.8 Hz, 2H). HRMS (ESI) m/z: $[M + H]^+$ calcd for $C_{97}H_{82}NO_{21}$, 1597.5408; found, 1597.5484.

$_CBABB_H$. The resin (50 mg, 90 μmol/g loading) functionalized with **$_CBBBA_{TMS}$** was cleaved and purified according to the procedure outlined above, and **$_CBBBA_{TMS}$** (4.0 mg, 2.5 μmol, 56% yield) was afforded as a white solid. ^{1}H NMR (400 MHz, $CDCl_3$ with 0.5% TFA and 0.1% H_2O): δ 9.99 (s, 1H), 9.98 (s, 1H), 9.95 (s, 1H), 8.23−8.14 (overlap, 6H), 8.09 (t, J = 1.6 Hz, 1H), 8.07−7.95 (overlap, 9H), 7.95−7.90 (overlap, 4H), 7.83 (s, 1H), 7.77 (t, J = 1.5 Hz, 1H), 7.58−7.54 (overlap, 2H), 4.62−4.51 (overlap, 8H), 3.97−3.88 (overlap, 8H), 3.85−3.76 (overlap, 8H), 3.76−3.69 (overlap, 8H), 3.49−3.47 (overlap, 9H), 3.47 (s, 3H), 3.22 (s, 1H), 2.63 (t, J = 7.3 Hz, 2H), 2.55 (t, J = 6.9 Hz, 2H), 1.99 (tt, J = 7.3, 6.9 Hz, 2H). HRMS (ESI) m/z: $[M + Na]^+$ calcd for $C_{97}H_{81}NO_{21}Na$, 1619.5227; found, 1619.5234.

■ ASSOCIATED CONTENT

Supporting Information

The Supporting Information is available free of charge at https://pubs.acs.org/doi/10.1021/acs.joc.0c01977.

NMR spectra and LCMS chromatograms (PDF)

■ AUTHOR INFORMATION

Corresponding Author

Jack W. Szostak − *Howard Hughes Medical Institute, Department of Molecular Biology and Center for Computational and Integrative Biology, Massachusetts General Hospital, Boston, Massachusetts 02114, United States; Department of Genetics, Harvard Medical School, Boston, Massachusetts 02115, United States; Department of Chemistry and Chemical Biology, Harvard University, Cambridge, Massachusetts 02138, United States;* orcid.org/0000-0003-4131-1203; Email: szostak@molbio.mgh.harvard.edu

Author

Kyle R. Strom − *Howard Hughes Medical Institute, Department of Molecular Biology and Center for Computational and Integrative Biology, Massachusetts General Hospital, Boston, Massachusetts 02114, United States; Department of Genetics, Harvard Medical School, Boston, Massachusetts 02115, United States;* orcid.org/0000-0002-0567-347X

Complete contact information is available at: https://pubs.acs.org/10.1021/acs.joc.0c01977

Notes

The authors declare no competing financial interest.

■ ACKNOWLEDGMENTS

The authors thank Dr. Noam Prywes for his thoughts and helpful comments on this manuscript, as well as the Szostak laboratory members for useful discussions. This work was supported by a grant (290363) from the Simons Foundation to J.W.S. J.W.S. is an Investigator of the Howard Hughes Medical Institute.

■ REFERENCES

(1) Watson, J. D.; Crick, F. H. C. Molecular Structure of Nucleic Acids: A Structure for Deoxyribose Nucleic Acid. *Nature* **1953**, *171*, 737−738.

(2) Ma, Q.; Lee, D.; Tan, Y. Q.; Wong, G.; Gao, Z. Synthetic Genetic Polymers: Advances and Applications. *Polym. Chem.* **2016**, *7*, 5199−5216.

(3) Joyce, G. F. Nonenzymatic Template-Directed Synthesis of Informational Macromolecules. *Cold Spring Harbor Symposia on Quantitative Biology*; Cold Spring Harbor Laboratory Press, 1987; Vol. *52*, pp 41−51.

(4) Prywes, N.; Blain, J. C.; Del Frate, F.; Szostak, J. W. Nonenzymatic Copying of RNA Templates Containing All Four Letters Is Catalyzed by Activated Oligonucleotides. *Elife* **2016**, *5*, No. e17756.

(5) Jauker, M.; Griesser, H.; Richert, C. Copying of RNA Sequences without Pre-Activation. *Angew. Chem., Int. Ed.* **2015**, *54*, 14559−14563.
(6) Zhou, L.; O'Flaherty, D. K.; Szostak, J. W. Template-Directed Copying of RNA by Non-Enzymatic Ligation. *Angew. Chem.* **2020**, *132*, 15812−15817.
(7) Lutz, J.-F. 100th Anniversary of Macromolecular Science Viewpoint: Toward Artificial Life-Supporting Macromolecules. *ACS Macro Lett.* **2020**, *9*, 185−189.
(8) Strom, K. R.; Szostak, J. W.; Prywes, N. Transfer of Sequence Information and Replication of Diimine Duplexes. *J. Org. Chem.* **2019**, *84*, 3754−3761.
(9) Núñez-Villanueva, D.; Ciaccia, M.; Iadevaia, G.; Sanna, E.; Hunter, C. A. Sequence Information Transfer Using Covalent Template-Directed Synthesis. *Chem. Sci.* **2019**, *10*, 5258−5266.
(10) Kamonsutthipaijit, N.; Anderson, H. L. Template-Directed Synthesis of Linear Porphyrin Oligomers: Classical, Vernier and Mutual Vernier. *Chem. Sci.* **2017**, *8*, 2729−2740.
(11) Lin, N.-T.; Lin, S.-Y.; Lee, S.-L.; Chen, C.-h.; Hsu, C.-H.; Hwang, L. P.; Xie, Z.-Y.; Chen, C.-H.; Huang, S.-L.; Luh, T.-Y. From Polynorbornene to the Complementary Polynorbornene by Replication. *Angew. Chem.* **2007**, *119*, 4565−4569.
(12) Zhou, Z.; Palermo, E. F. Templated Ring-Opening Metathesis (TROM) of Cyclic Olefins Tethered to Unimolecular Oligo (Thiophene) s. *Macromolecules* **2018**, *51*, 6127−6137.
(13) Laurent, E.; Amalian, J.-A.; Parmentier, M.; Oswald, L.; Al Ouahabi, A.; Dufour, F.; Launay, K.; Clément, J.-L.; Gigmes, D.; Delsuc, M.-A.; et al. High-Capacity Digital Polymers: Storing Images in Single Molecules. *Macromolecules* **2020**, *53*, 4022.
(14) Lee, J. M.; Koo, M. B.; Lee, S. W.; Lee, H.; Kwon, J.; Shim, Y. H.; Kim, S. Y.; Kim, K. T. High-Density Information Storage in an Absolutely Defined Aperiodic Sequence of Monodisperse Copolyester. *Nat. Commun.* **2020**, *11*, 56.
(15) Elliott, E. L.; Ray, C. R.; Kraft, S.; Atkins, J. R.; Moore, J. S. Solid-Phase Synthesis of m-Phenylene Ethynylene Heterosequence Oligomers. *J. Org. Chem.* **2006**, *71*, 5282−5290.
(16) Young, J. K.; Nelson, J. C.; Moore, J. S. Synthesis of Sequence Specific Phenylacetylene Oligomers on an Insoluble Solid Support. *J. Am. Chem. Soc.* **1994**, *116*, 10841−10842.
(17) Zhang, J.; Moore, J. S.; Xu, Z.; Aguirre, R. A. Nanoarchitectures. 1. Controlled Synthesis of Phenylacetylene Sequences. *J. Am. Chem. Soc.* **1992**, *114*, 2273−2274.
(18) Szweda, R.; Chendo, C.; Charles, L.; Baxter, P. N. W.; Lutz, J.-F. Synthesis of Oligoarylacetylenes with Defined Conjugated Sequences Using Tailor-Made Soluble Polymer Supports. *Chem. Commun.* **2017**, *53*, 8312−8315.
(19) Hartley, C. S.; Elliott, E. L.; Moore, J. S. Covalent Assembly of Molecular Ladders. *J. Am. Chem. Soc.* **2007**, *129*, 4512−4513.
(20) Leguizamon, S. C.; Scott, T. F. Sequence-Selective Dynamic Covalent Assembly of Information-Bearing Oligomers. *Nat. Commun.* **2020**, *11*, 784.
(21) Hebel, M.; Riegger, A.; Zegota, M. M.; Kizilsavas, G.; Gačanin, J.; Pieszka, M.; Lückerath, T.; Coelho, J. A. S.; Wagner, M.; Gois, P. M. P.; et al. Sequence Programming with Dynamic Boronic Acid/Catechol Binary Codes. *J. Am. Chem. Soc.* **2019**, *141*, 14026−14031.
(22) Giuseppone, N.; Schmitt, J.-L.; Schwartz, E.; Lehn, J.-M. Scandium (III) Catalysis of Transimination Reactions. Independent and Constitutionally Coupled Reversible Processes. *J. Am. Chem. Soc.* **2005**, *127*, 5528−5539.
(23) Matsumoto, M.; Dasari, R. R.; Ji, W.; Feriante, C. H.; Parker, T. C.; Marder, S. R.; Dichtel, W. R. Rapid, Low Temperature Formation of Imine-Linked Covalent Organic Frameworks Catalyzed by Metal Triflates. *J. Am. Chem. Soc.* **2017**, *139*, 4999−5002.
(24) Wei, T.; Furgal, J. C.; Scott, T. F. In Situ Deprotection and Dynamic Covalent Assembly Using a Dual Role Catalyst. *Chem. Commun.* **2017**, *53*, 3874−3877.
(25) Wei, T.; Furgal, J. C.; Jung, J. H.; Scott, T. F. Long, Self-Assembled Molecular Ladders by Cooperative Dynamic Covalent Reactions. *Polym. Chem.* **2017**, *8*, 520−527.
(26) Vologodskii, A.; Frank-Kamenetskii, M. D. DNA Melting and Energetics of the Double Helix. *Phys. Life Rev.* **2018**, *25*, 1−21.
(27) Wang, P.; Meyer, T. A.; Pan, V.; Dutta, P. K.; Ke, Y. The Beauty and Utility of DNA Origami. *Chem* **2017**, *2*, 359−382.
(28) Strobel, E. J.; Yu, A. M.; Lucks, J. B. High-Throughput Determination of RNA Structures. *Nat. Rev. Genet.* **2018**, *19*, 615−634.
(29) Sonogashira, K. Development of Pd−Cu Catalyzed Cross-Coupling of Terminal Acetylenes with Sp2-Carbon Halides. *J. Organomet. Chem.* **2002**, *653*, 46−49.
(30) Wuts, P. G.; Greene, T. W. *Greene's Protective Groups in Organic Synthesis*; John Wiley & Sons, 2006.
(31) Wagner, R. W.; Johnson, T. E.; Li, F.; Lindsey, J. S. Synthesis of Ethyne-Linked or Butadiyne-Linked Porphyrin Arrays Using Mild, Copper-Free, Pd-Mediated Coupling Reactions. *J. Org. Chem.* **1995**, *60*, 5266−5273.
(32) Ciaccia, M.; Di Stefano, S. Mechanisms of Imine Exchange Reactions in Organic Solvents. *Org. Biomol. Chem.* **2015**, *13*, 646−654.
(33) Belowich, M. E.; Stoddart, J. F. Dynamic Imine Chemistry. *Chem. Soc. Rev.* **2012**, *41*, 2003−2024.
(34) Cordes, E. H.; Jencks, W. P. The Mechanism of Hydrolysis of Schiff Bases Derived from Aliphatic Amines. *J. Am. Chem. Soc.* **1963**, *85*, 2843−2848.
(35) Godoy-Alcántar, C.; Yatsimirsky, A. K.; Lehn, J.-M. Structure-Stability Correlations for Imine Formation in Aqueous Solution. *J. Phys. Org. Chem.* **2005**, *18*, 979−985.
(36) HRMS (ESI) *m/z*: $[M + H]^+$ calcd for $C_{102}H_{87}N_2O_{20}$, 1660.5880; found, 1660.5439.
(37) To assure the NMR spectra obtained reflected kinetically stable populations, spectra were acquired immediately after D_2O addition and at 10 min and 1 h time points. In all cases, the spectra acquired immediately were identical to the later time points.
(38) Orgel, L. E. Unnatural Selection in Chemical Systems. *Acc. Chem. Res.* **1995**, *28*, 109−118.
(39) Letsinger, R. L.; Mahadevan, V. Oligonucleotide Synthesis on a Polymer Support1, 2. *J. Am. Chem. Soc.* **1965**, *87*, 3526−3527.
(40) Gilham, P. T.; Khorana, H. G. Studies on Polynucleotides. I. A New and General Method for the Chemical Synthesis of the C5 ″-C3 ″internucleotidic Linkage. Syntheses of Deoxyribo-Dinucleotides1. *J. Am. Chem. Soc.* **1958**, *80*, 6212−6222.
(41) Sankar, M.; Nowicka, E.; Carter, E.; Murphy, D. M.; Knight, D. W.; Bethell, D.; Hutchings, G. J. The Benzaldehyde Oxidation Paradox Explained by the Interception of Peroxy Radical by Benzyl Alcohol. *Nat. Commun.* **2014**, *5*, 3332.

https://dx.doi.org/10.1021/acs.joc.0c01977
J. Org. Chem. 2020, 85, 13929−13938